INFLUENCE OF EXTRUDER PLASTICIZING SYSTEMS
ON THE SELECTED PROPERTIES OF PLA/GRAPHITE COMPOSITE

Daniel KACZOR*,** [ID], **Krzysztof BAJER*** [ID], **Grzegorz DOMEK**** [ID]
Piotr MADAJSKI*** [ID], **Aneta RASZKOWSKA-KACZOR*** [ID], **Paweł SZROEDER****** [ID]

*Łukasiewicz Research Network Institute for Engineering of Polymer Materials and Dyes,
Marii Skłodowskiej-Curie 55, 87-100 Toruń, Poland
**Faculty of Mechatronics, Kazimierz Wielki University, Kopernika 1, 85-074 Bydgoszcz, Poland
***Faculty of Chemistry, Nicolaus Copernicus University, Gagarina 7, 87-100 Toruń, Poland
****Institute of Physics, Kazimierz Wielki University, Powstańców Wielkopolskich 2, 85-090 Bydgoszcz, Poland

daniel.kaczor@impib.lukasiewicz.gov.pl, krzysztof.bajer@impib.lukasiewicz.gov.pl, gdomek@ukw.edu.pl
piotr.madajski@doktorant.umk.pl, aneta.kaczor@impib.lukasiewicz.gov.pl, psz@ukw.edu.pl

Abstract: Twin-screw extrusion is a crucial method for the direct inserting of carbon micro- and nanomaterials into a polymer matrix using a dry procedure. The study aimed to determine the influence of the parameters of the twin-screw extruder plasticizing system on the dispersion homogeneity and distribution of graphite filler in the polylactide polymer matrix and overall quality of the composite. As a filler, a graphite micropowder with a 5 μm lateral size of platelets was used at concentration of 1 wt.%. Three configurations of screws with different mixing intensity and various types segments were considered in the extrusion experiments. Morphology and chemical structure of the obtained composites were examined using scanning electron microscopy (SEM), Fourier transform infrared spectroscopy – attenuated total reflectance (FTIR-ATR) and Raman spectroscopy. Differential scanning calorimetry (DSC) and melting flow rate measurements (MFR) were used to asses thermal and rheological properties of the composites. Samples of the polylactide/graphite composites were also subjected to mechanical tests. The results show that the selection of the mechanical parameters of twin-screw extruder plasticizing system plays a key role in the preparation of the homogeneous PLA/graphite composites. Incorrect selection of the screw geometry results in poor mixing quality and a significant deterioration of the mechanical and thermal properties of the composites. Optimised mixing and extrusion parameters can be the starting point for the design of efficient twin-screw extruder plasticizing system for fabrication of PLA composites with carbon nanotube and graphene fillers.

Key words: differential scanning calorimetry, extrusion, graphite, infrared spectroscopy, mechanical properties, melting flow rate, plasticizing system, polylactide, twin-screw extruder

1. INTRODUCTION

Traditional polymers, obtained from crude oil, are nowadays increasingly being replaced by their equivalents produced from renewable sources. Their use reduces environmental pollution, greenhouse gas emissions and the consumption of fossil resources [1–6]. Polylactide (PLA), also known as poly(lactic acid), is the oldest and one of the most interesting and useful biodegradable polymers. Currently, PLA has a principal position on the market of biodegradable polymers [7]. Several applications of PLA-based polymers have been developed in the automotive [8, 9], agricultural [10, 11], medicine [12, 13], electronic [14, 15] and packaging [16, 17] industries.

To improve mechanical, thermal and electrical properties of PLA for industrial and commodity applications, various types of fillers have been added: nanomaterials [18], organic fibres [19], talc [20], montmorillonite [21] and graphite [22]. Carbon nanomaterials such as carbon nanotubes and graphene with superior thermal and electrical properties can be used as a filler that improves some specific properties, such as stiffness, thermal stability, fire retardancy and lower permeability [23].

Due to its high versatility, PLA is processed using the same methods as other popular polymers: injection and compression moulding, spinning, extrusion or 3D printing [24–28].

Extrusion has been widely used in the manufacture of films, sheets, pipes and profiles. This processing technique can be used for preparation of polylactide composites containing a wide range of additives. The advantages of the extrusion include high efficiency, quality and repeatability, and possibility of mass production and of obtaining multi-component composites in one technological process. The quality and thus the properties of polymer composites obtained by extrusion are affected by both the extrusion temperature [29] and processing speed [30]. The configuration of the extruder plasticizing system plays a key role in the dispersion quality of the filler in the polymer matrix and the properties of final composites [31]. High-quality polymer composites are characterised by an excellent dispersion of the filler. Undispersed filler agglomerates exercised a negative effect on mechanical [32], thermal [33] and electrical properties [34] of obtained composites.

Good dispersion can be obtained using plasticizing systems characterised by high mixing and grinding abilities. However, the use of such systems may have a negative effect in terms of change in the degree of polymer degradation [35].

The innovation of work involves the selection of an optimal

plasticizing system of a twin-screw extruder with the preferred processing parameters required to obtain PLA composites with an excellent dispersion of graphite fillers and without significant changes in polymer properties. The developed system will be used for further research on composites with carbon nanotubes and graphene as similar fillers. Currently, there is little information on the optimal configuration of screws in the processing of PLA with carbon fillers of this type.

2. MATERIALS AND SAMPLE PREPARATION

Graphite micropowder, MG3096 (3000 mesh), used as a carbon filler, was purchased from Sinograf S.A. Company (Poland). The polylactide (PLA) produced by Total-Corbion (Netherlands), available under the trade name Luminy® LX175 (sample marked as PLA/TC), was used as a matrix in the obtained polymer masterbatches and composites. For obtaining masterbatches, before mixing, PLA was ground into powder form with a particle size of 100–600 µm. Typical properties of used PLA are shown in Table 1 [36, 37].

Tab. 1. Typical properties of Luminy® LX175

Properties	Method	Typical value
Density	Literature value	1.24 g/cm^3
Stereochemical purity	Total-Corbion PLA method	96% (L-isomer)
Residual monomer	Total-Corbion PLA method	≤0.3%
Melting temperature	DSC	155 °C
Glass transition temperature	DSC	60 °C

2.1. Masterbatch preparation

Masterbatch was prepared by mixing 30 g of polylactide with 10 g of graphite powder in a mixer (50 EHT Brabender Plasti-Corder® Lab-Station Germany), at 190 °C and 50 rpm.

Before the mixing process, PLA was dried in the POL-EKO SLW 180 STD dryer at temperature 80 °C for 8 h. Preparation of the masterbatch in the mixer was carried out in two stages. In the first, PLA was melted for 2.5 min; in the second, graphite powder was added and the mixture was stirred for 2 min. The properties of obtained masterbatch are available in our published papers [38, 39].

2.2. Composites preparation

The tested composites containing 1% graphite were extruded using 960 g of pristine PLA with 40 g of masterbatch. The extrusion process was carried out using a twin-screw extruder (Bühler BTSK, Uzwil, Switzerland) with a screw diameter of 20 mm and a screw length of 790 mm. All samples were extruded at the same main drive speed: 150 rpm; and temperature profile: 180 °C, 180 °C, 190 °C, 190 °C or 195 °C (head). The following parameters were registered during the extrusion process: changes of the temperature in each extruder zone, stock temperature, torque of the main drive, power of the main drive and the process efficiency. Before extrusion, polylactide and masterbatch were dried in a

dryer for 8 h at 80 °C. Three configurations of screws with different mixing intensities and various types of mixing segments were used to prepare samples.
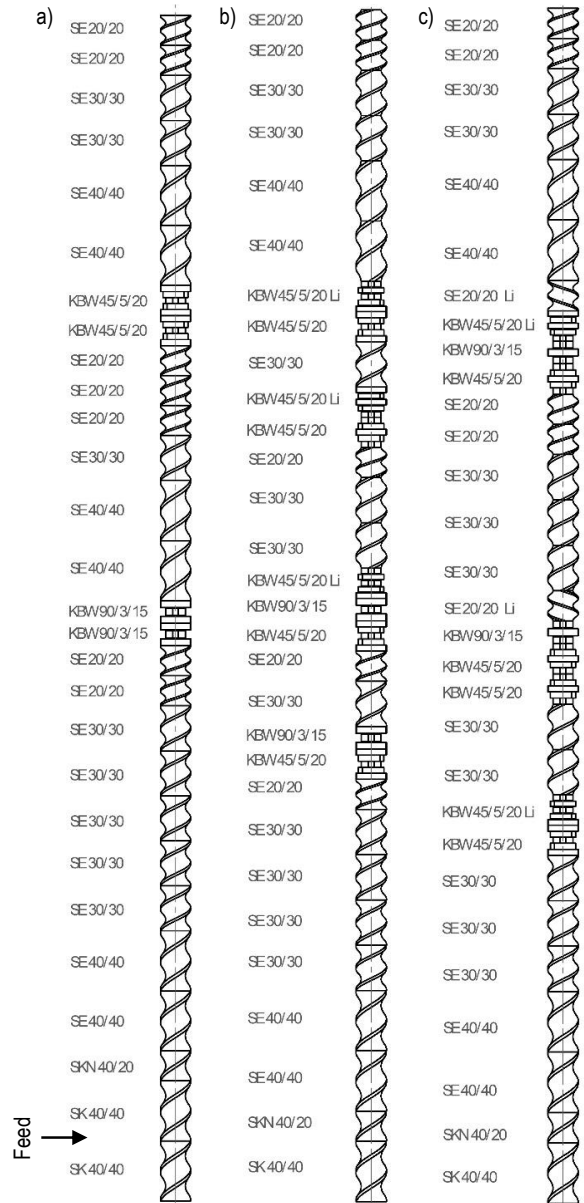

Fig. 1. Drawings of the screw systems: (A) K1; (B) K3; (C) K5

The K1 system, shown in Figure 1A, is characterised by two zones with low intensity mixing and shearing functions. In the first zone, two neutral kneading elements KBW 90/3/15 were used and in the second zone, two forward kneading elements KBW 45/5/20 were used.

The K3 screw system shown in Figure 1B has a higher intensity than the K1 system, and it includes four mixing and shearing zones. The first zone of the screw system consists of two kneading elements KBW 90/2/15 and KBW 45/5/20. The subsequent zones have forward kneading elements and an additional reverse kneading element KBW 45/5/20. The reverse element holds the polymer in the zone for longer, resulting in more intense mixing, but this can lead to the degradation of PLA.

K5, shown in Figure 1C, is a strong mixing and degrading system. We included this in our study to observe the effect of strong

mixing on PLA matrix. The system includes three mixing–shearing zones. Each one contains a reverse kneading element, which causes a significant increase in mixing.

Neat polymers (PLA/NG) and polylactide-graphite composites (PLA/G) prepared using one of the three plasticizing systems (K1, K3, or K5) are listed in Table 2.

Tab. 2. Labelling and processing methods of PLA/graphite composites

Sample	Graphite content (%)	Plasticizing system
PLA/NG/K1	0	K1
PLA/G/K1	1	K1
PLA/NG/K3	0	K3
PLA/G/K3	1	K3
PLA/NG/K5	0	K5
PLA/G/K5	1	K5

3. MATERIALS CHARACTERISATION

3.1. Phase morphology analysis

To evaluate the dispersion of graphite in the polymer matrix, scanning electron microscopy (SEM, SU8010, Hitachi, Japan) was used. For SEM imaging, samples were deposited on conductive carbon adhesive tape and coated with a nanometrical layer of gold. Gold was used to increase the surfaces' electrical conductivity in the tested samples. All microscopic observations were made at the accelerating voltage of 10 kV and a working distance of 8 mm.

3.2. Chemical structure analysis

Fourier transform infrared spectroscopy – attenuated total reflectance spectra were measured using the Cary 630 FTIR-ATR spectrometer (Agilent Technologies, USA). Measurements were carried out over the spectral range of 400–4000 cm⁻¹ with a resolution of 2 cm⁻¹.

Raman spectra were recorded in backscattering geometry, with a Senterra Raman microscope (Bruker Optik, Billerica, MA, USA), using a 2-mW laser beam with a wavelength of 532 nm as an excitation light source.

Both the FTIR-ATR and Raman spectra were acquired at ambient temperatures.

3.3. Thermal behaviour and stability analysis

The Mettler Toledo (Switzerland) DSC1 calorimeter was used to perform differential scanning calorimetry. The calorimeter was calibrated with pure indium and zinc standards. All samples were tested under nitrogen atmosphere, at a gas flow rate of 50 cm³/min. Each sample of 5–7 mg was sealed in aluminium crucible. DSC analysis was divided into five stages:
- First stage (heating 1): the samples were heated at a constant rate of 10 °C/min from 0 °C to 300 °C.
- Second stage: this was an isothermal stage lasting 5 min.

- Third stage: the samples were cooled at a rate of 10 °C/min to 0 °C.
- Fourth stage: this was an isothermal stage lasting 5 min.
- Fifth stage (heating 2): the samples were heated at a constant rate of 10 °C/min from 0 °C to 300 °C.

The analyses were performed in accordance with the PN-EN ISO 11357-(1-3): 2009 standards [40].

The decomposition temperature of the Luminy® LX175 in nitrogen atmosphere is above 300 °C [41].

The room temperature crystallinity, X_C (1), of PLA composites was evaluated using the following formula:

$$X_C = \left(\frac{\Delta H_m - \Delta H_{cc}}{w \Delta H_m^0}\right) \cdot 100\% \qquad (1)$$

where X_C represents PLA crystallinity, ΔH_m melting enthalpy, ΔH_{cc} cold crystallisation enthalpy (J/g), w fraction of the polymer in the composite materials and ΔH_m^0 melting enthalpy of 100% crystalline PLA (93 J/g) [42].

3.4. Rheological properties

The melt flow rate of the composites was determined according to the PN-EN ISO 1133:2011 standard [43] using a Dynisco (USA) LMI 4003 capillary plastometer. The measurements were carried out under the piston loading of 2.16 kg at 190 C. Samples were dried before measurement for 8 h at 80 °C in a drier.

3.5. Mechanical properties

To perform tensile and Charpy impact tests, normalised dumbbells and bars were prepared using a laboratory injection moulding type Plus 35 (Battenfeld GmbH, Germany). The moulded pieces were made according to PN-EN ISO 294-1 standard [44].

To determine tensile strength (σ_m), stress at break (σ_b), strain at strength (ε_m) and elongation at break (ε_b) according to the PN-EN ISO 527-1:2020 standard [45], a tensile testing machine type TIRAtest 27025 (TIRA Maschinenbau GmbH, Germany) was used. The mechanical properties were measured at a speed of 50.0 mm/min. Tensile modulus (E_t) was determined with the use of the same machine at a speed of 1.0 mm/min.

Charpy impact strength (α_{cN}) was determined in notched samples type 1eU according to the PN-EN ISO 179-1:2010 standard [46] with edgewise impact, using a pendulum impact tester, type IMPats15 (ATS FAAR, Italy), equipped with a 0.5-N pendulum.

All mechanical tests were carried out at 50% relative humidity and 23 °C. The specimens were conditioned in the same conditions as the measurement for 24 h.

4. RESULTS

4.1. Extrusion process analysis

Table 3 shows the values of stock temperature (T_t), torque main drive (M_o), power main drive (W) and efficiency (Y) recorded during extrusion.

Tab. 3. Parameters recorded during extrusion

Sample	PLA/NG/K1	PLA/G/K1	PLA/NG/K3	PLA/G/K3	PLA/NG/K5	PLA/G/K5
T_t (°C)	220	220	217	220	218	218
M_o (Nm)	15.5	16.5	21.5	22.0	25.7	26.4
W (kW)	0.46	0.47	0.65	0.66	0.74	0.76
Y (kg/h)	3.7	3.7	3.7	3.7	3.7	3.7

The K1 system generated low torque in the range of 15.5–16.5 Nm. The increase in mixing intensity resulted in an increase in torque by almost 21.5 Nm (K3) and by as much as 25.7 Nm in the case of K5. Changes in the value of the main drive power supply, which were related to the increased mixing capacity of the plasticizing system, were also observed. The value of this parameter for K1 is lower than for K5 by 62%. No differences between the set and actual extrusion temperature were observed. The addition of 1% graphite did not cause any significant differences in the extrusion process. The only observed differences were a slight increase in the torque and power main drive in samples with graphite filler compared to the neat polymer samples extruded in this same plasticizing system. Addition of graphite and changes in plasticizing system have not resulted in changes in the efficiency of the process.

4.2. Phase morphology analysis

Figure 2 shows SEM images of graphite fillers and PLA graphite composites, and the size of the graphite flakes was found to be 6 ± 2 μm. In the breakthrough of the sample obtained with the K1 plasticizing system, the presence of larger fragments of graphite filler is visible. This means that the graphite introduced into the polymer matrix was not completely ground during extrusion. The graphite filler in the PLA/G/K3 and PLA/G/K5 samples was rubbed into smaller pieces, and this proves that better mixing and grinding properties of screws were utilised in the K3 and K5 systems compared with K1. For the samples obtained with the use of K3 and K5 plasticizing systems, orientation of the graphite flakes in the direction of extrusion can be seen.

No pores or any other types of discontinuity were found in the polymer matrix.

4.2. FTIR-ATR and Raman analyses

Figure 3 shows FTIR-ATR spectra of the composites. The lowest spectrum was obtained for the raw PLA (PLA/TC sample). Recorded absorption spectra contain the bands assigned to the PLA polymer matrix [47, 48]. The crystalline and amorphous polymer phases can be assigned to bands at 753 cm^{-1} and 865 cm^{-1}. At 1041 cm^{-1} appear the stretching modes of C–CH$_3$ group. The symmetric and asymmetric stretching modes of the C–O–C group appear at 1081 cm^{-1} (symm), 1180 cm^{-1} and 1266 cm^{-1}, respectively, while 1127 cm^{-1} is a position of rocking modes of the CH$_3$ group band. Features characteristic to the CH and CH$_3$ sym-

metric bending modes appear at 1358 cm^{-1} and 1381 cm^{-1}, while the band corresponding to the asymmetric bending modes is found at 1452 cm^{-1}. Ester C=O stretching modes appear at 1746 cm^{-1}. Weak bands (not shown in Figure 4) at 2945 cm^{-1} and 2994 cm^{-1} are attributed to the asymmetric modes of the CH$_3$ group.
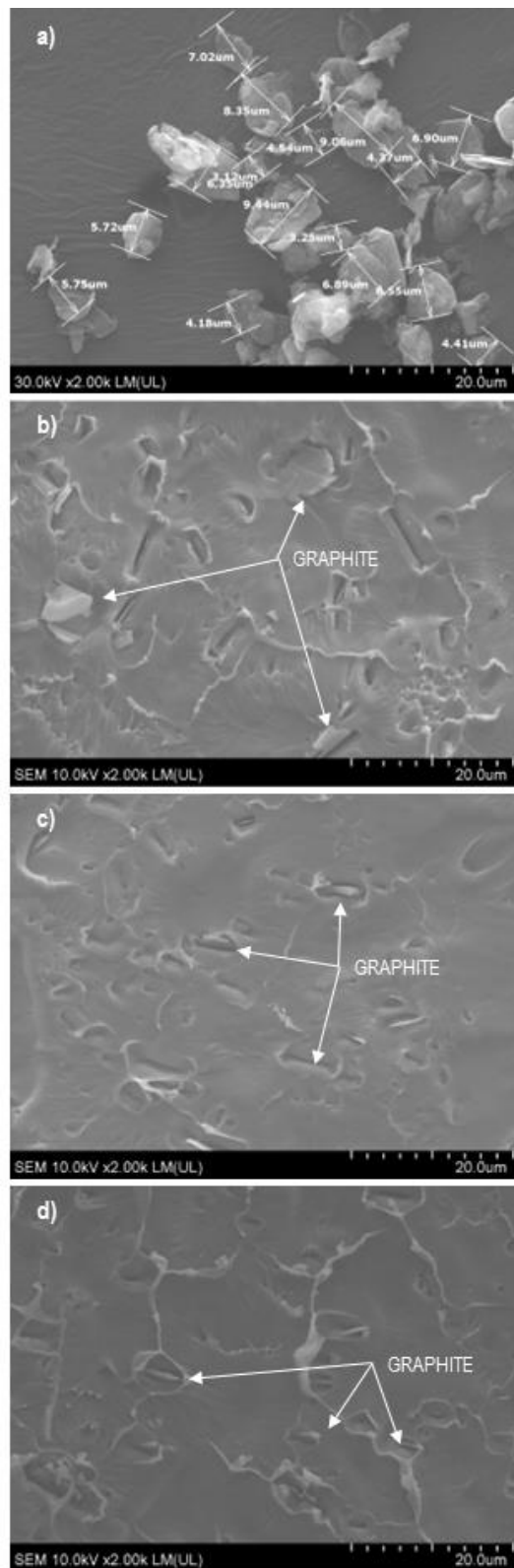

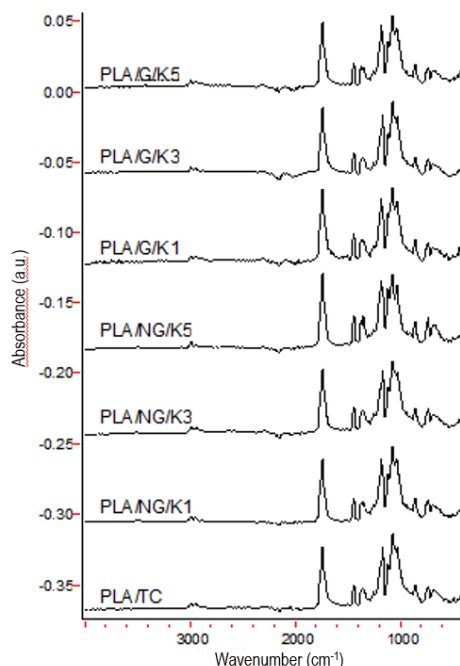**Fig. 2.** SEM picture of: (A) graphite filler, samples; (B) PLA/G/K1; (C) PLA/G/K3; (D) PLA/G/K5

Fig. 3. FTIR-ATR spectra of samples

The plasticizing system used during extrusion did not change the intensity of the bands assigned to the carbonyl (1746 cm⁻¹) and ester (1081 cm⁻¹ and 1180 cm⁻¹) groups. The changes in intensity (reduction) of these peaks indicates the shortening of the polymer chains and thus their degradation [49]. Based on this observation, it can be concluded that the used plasticizing systems did not cause polylactide degradation, or caused only a negligibly low amount of degradation.

Graphite filler does not affect the position and relative intensities of the characteristic PLA bands.
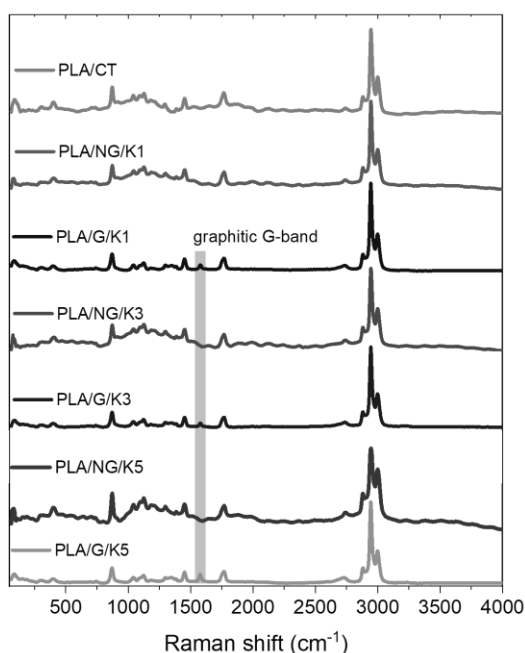

Fig. 4. Raman spectra of neat PLA and PLA/graphite composites

As shown in Figure 4, various oscillation modes visible in FTIR-ATR are also Raman-active. These include the following

bands: the stretching modes of the C-CH₃ group at 1042 cm⁻¹, symmetric stretching modes of C-O-C group at 1092 cm⁻¹, the rocking modes of the CH₃ group at 1127 cm⁻¹ and the asymmetric bending modes of the CH₃ group at 1452 cm⁻¹. The ester C=O group stretch shows a complex band at around 1770 cm⁻¹. As Qin and Kean [50] have demonstrated, in amorphous PLA, the single C=O stretching mode appears at 1770 cm⁻¹, whereas in crystalline polymer triplet band it is present at 1776 cm⁻¹, 1766 cm⁻¹ and 1750 cm⁻¹. Results of the C=O band deconvolution show significant decrease of the 1750 cm⁻¹ component intensity in samples subjected to plasticizing process, which indicates reduction of the crystallinity. However, no differences are observed between the proceeded samples of neat polymer and composite. Additionally, the choice of the screw system does not affect the C=O band structure.

Compared to the FTIR-ATR bands, the bands assigned to symmetric stretching of the CH₃ group at 2881 cm⁻¹ and 2945 cm⁻¹, and asymmetric stretching of the methyl group at 2998 cm⁻¹, are very strong.

Raman feature at 873 cm⁻¹, attributed to the stretching modes of the C–COO group of PLA, is seen.

Graphitic G-band appears at 1578 cm⁻¹ in samples PLA/G/K1, PLA/G/K3 and PLA/G/K5 containing graphite filler.

4.3. Thermal behaviour and stability analysis

To determine the influence of the extruder screws' configuration on the thermal properties of the obtained composites, the DSC technique was used. Thermal data, such as the glass transition temperature (T_g), crystallisation temperature (T_c), cold crystallisation temperature (T_{cc}), melting temperature (T_m), crystallisation enthalpy (ΔH_c), cold crystallisation enthalpy (ΔH_{cc}) and melting enthalpy (ΔH_m), are summarised in Table 4. Thermograms for the first and second heating scans are presented in Figures 5 and 6, respectively.

The heating scan of the pristine PLA (sample PLA/TC) showed an endothermic peak corresponding to the melting of the polymer ($T_m{}^1$ = 148.8 °C). This peak was not observed in the second heating scan. This behaviour confirms that the slow crystallisation rate of high molecular weight PLA is not conducive to the development of the crystalline phase during cooling [51]. The rate used during the cooling of the polymer melt (10 °C/min) does not allow for recrystallisation. This speed is too fast for the polylactide chains to reorganise into crystal regions. Since the mobility of the chains is not limited by the presence of crystallites, the glass transition (compared to heating 1) is more pronounced [52]. The absence/large reduction of this peak has also been reported by other researchers [53–55].

For all samples, the glass transition between 57 °C and 64 °C (heating 1) marks the point at which the polymer chains are allowed to move. Reorganisation of amorphous domains into crystalline ones manifest as an exothermic peak at 111 °C in the case of neat polymer and 116–117 °C for PLA/graphite composite. The increase in temperature is related to the restriction of the mobility of the polymer chains by graphite micro-platelets, which hinders the formation of a semi-crystalline phase in the polymer [56]. Melting peak appears near 151–153 °C. There is no correlation between graphite content and melting enthalpy in heating 1 scan results. All samples have amorphous character.

Tab. 4. Thermal parameters obtained by DSC

Sample	PLA/TC	PLA/NG/K1	PLA/G/K1	PLA/NG/K3	PLA/G/K3	PLA/NG/K5	PLA/G/K5
Heating 1							
T_m^1 (°C)	148.8	151.4	153.5	151.4	151.8	151.7	153.2
ΔH_m^1 (J/g)	28.7	28.2	24.3	25.8	26.8	26.6	27.1
T_g^1 (°C)	64.3	58.0	60.2	61.5	61.5	58.8	57.6
$T_{cc}1$ (°C)	-	111.5	117.3	111.7	115.9	112.0	117.3
ΔH_{cc}^1 (J/g)	-	27.7	24.1	26.6	26.1	26.6	27.0
X_c^1 (%)	31	0	0	0	0	0	0
Heating 2							
T_m^2 (°C)	-	151.3	151.2	151.5	150.1	151.1	150.0
ΔH_m^2 (J/g)	-	3.1	15.4	2.1	22.7	10.6	24.0
T_g^2 (°C)	57.1	58.7	60.0	59.1	59.0	59.1	59.8
T_{cc}^2 (°C)	-	131.3	128.1	129.8	125.4	129.3	125.3
ΔH_{cc}^2 (J/g)	-	3.0	15.1	1.8	22.5	10.3	23.8
X_c^2 (%)	0	0	0	0	0	0	0

Fig. 6. Heating 2 DSC thermograms of samples

Glass transition temperature in the second heating scan is almost in this same level, near 60 °C, for all samples. The same observation can be made in the case of the melting temperature, where, too, the differences between the samples are small. However, there is a difference in the melting enthalpy between PLA/graphite composites and neat polymers. Samples with graphite filler need much more energy to melt. The same relationship occurs with regard to the enthalpy and temperature of cold crystallisation. For samples with graphite, ΔH_{cc}^2 is higher and T_{cc}^2 lower. Graphite fillers affect the position of the exothermic peak, which is slightly shifted to lower temperatures. As revealed by molecular simulations, local mobility of the polymer chains near the graphite phase are highly anisotropic and drastically reduced in the direction perpendicular to the graphite basal planes. Thus, graphite filler can act as a nucleating agent that promotes the crystallisation process. As a consequence, the T_{cc}^2 decreases [57]. Crystallinity determined from the second heating data for all samples is on a 0% level.

4.4. Rheological properties

Table 5 summarises the MFR values of the obtained samples. An increase in MFR value may be a sign of degradation of the polymer [58]. In the samples without graphite, no significant increase in the value of this parameter was observed. This observation, combined with the conclusions from the FTIR-ATR analysis, allows us to suppose that the used plasticizing system had a negligible effect on the degradation of the used PLA. For samples containing graphite, a slight increase in the melt flow rate can be noticed compared to the samples without this additive, obtained with the same plasticizing system. This may be due to an increase in flow resistance associated with the use of solid filler [59].

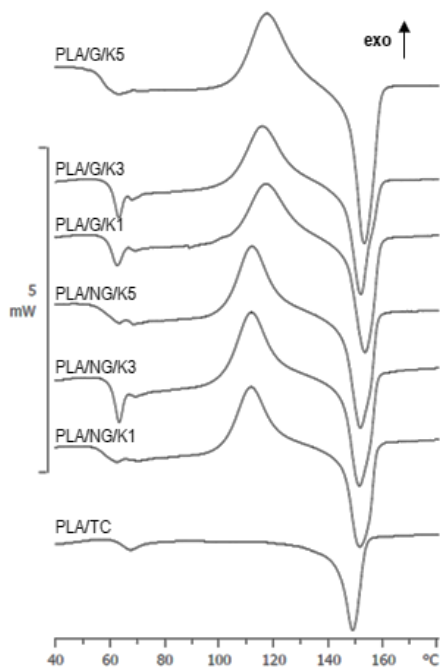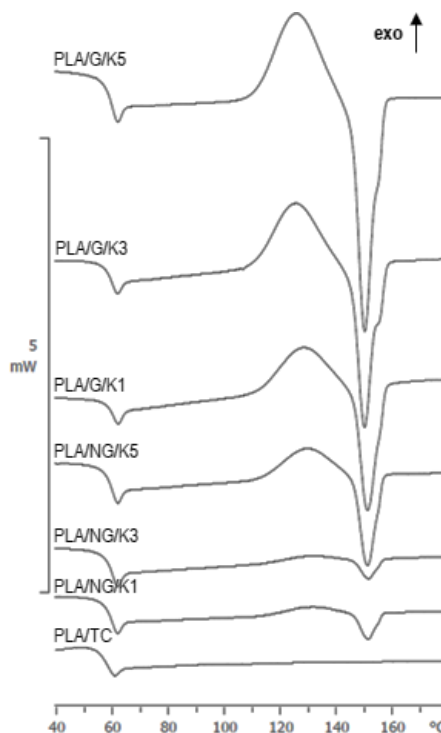**Fig. 5.** Heating 1 DSC thermograms of samples

No changes were recorded on the thermograms of the samples during cooling.

Daniel Kaczor, Krzysztof Bajer, Grzegorz Domek, Piotr Madajski, Aneta Raszkowska-Kaczor, Paweł Szroeder
Influence of Extruder Plasticizing Systems on the Selected Properties of PLA/Graphite Composite

DOI 10.2478/ama-2022-0038

Tab. 5. MFR values with standard deviations

Sample	MFR [g/10 min]
PLA/NG/K1	5.8 ± 0.2
PLA/G/K1	5.8 ± 0.1
PLA/NG/K3	6.3 ± 0.1
PLA/G/K3	6.0 ± 0.1
PLA/NG/K5	6.4 ± 0.1
PLA/G/K5	6.0 ± 0.1

4.5. Mechanical properties

The results of mechanical tests of the samples are summarised in Table 6.

Tab.6. Mechanical properties

Sample	PLA/TC	PLA/NG/K1	PLA/G/K1	PLA/NG/K3	PLA/G/K3	PLA/NG/K5	PLA/G/K5
Static tension							
σ_m (MPa)	71.8 ± 0.6	65.3 ± 2.7	64.0 ± 2.9	67.3 ± 2.3	63.3 ± 1.9	67.6 ± 0.7	63.5 ± 1.1
σ_b (MPa)	70.9 ± 1.6	65.2 ± 2.5	63.7 ± 2.7	67.0 ± 2.3	63.0 ± 1.8	67.4 ± 0.7	63.0 ± 1.0
ε_m (%)	4.7 ± 0.2	4.3 ± 0.2	4.1 ± 0.2	4.4 ± 0.4	4.2 ± 0.2	4.7 ± 0.1	4.3 ± 0.1
ε_b (%)	5.1 ± 0.4	4.4 ± 0.2	4.2 ± 0.2	4.4 ± 0.4	4.3 ± 0.2	4.7 ± 0.1	4.4 ± 0.1
E_t (MPa)	3135 ± 82	2024 ± 124	2168 ± 79	2193 ± 125	2101 ± 81	1943 ± 82	2024 ± 156
Charpy impact strength							
α_{cN} (kJ/m^2)	2.9 ± 0.3	3.2 ± 0.4	3.5 ± 0.3	2.8 ± 0.2	2.9 ± 0.1	2.4 ± 0.1	3.3 ± 0.2

During extrusion, the polylactide is partially degraded [58]. This can be observed by comparing the mechanical properties registered during static tension between the pristine polylactide and the samples obtained by a twin-screw extruder without graphite. For these samples, correlations are not observed between the plasticizing system used and changes in mechanical properties. This means that the high temperature associated with the composite extrusion process is mainly responsible for the degradation of the polymer. It should also be taken into account that the samples made of the granulate obtained with the twin-screw extruder were subjected to one thermal treatment more than PLA. An additional process could increase the degradation of the polymer, which is manifested by a greater difference in the values recorded during the static tensile tests.

The addition of graphite caused a slight reduction in value of tensile strength (σ_m) and stress at break (σ_b) for all samples. The same effect was observed by other researchers [60–62].

The results of the Charpy impact test do not show any significant difference between samples. It seems that the configuration of the plasticizing system does not affect the value of this parameter. The addition of graphite microplates slightly increased the value of Charpy impact strength. Polymer degradation can be responsible, among other things, for the decrease in the α_{cN} value [63]. Since the difference between the PLA/TC sample and the others is small, it can be concluded that the polymer degradation during extrusion is insignificant.

5. CONCLUSIONS

The configuration of the plasticizing system of the twin-screw extruder affects the properties of the obtained polymer composites. For efficient mixing of the composite, it is necessary to use a screw with intensive mixing system. The mild configuration makes it impossible to obtain composites with an effective dispersion of graphite in the polymer matrix. The systems equipped with segments responsible for improving mixing, grinding and reversing the material ensure proper grinding of the graphite flakes and prevent the formation of agglomerates.

However, the increase in mixing intensity generates a greater load on the machine (M_o and W); therefore, the mixing and grinding elements in the screw system should be optimally selected to obtain the correct graphite dispersion with the lowest possible load on the machine during processing.

The increase in the intensity of mixing and shear in the screw configuration causes slight degradation in the PLA chain (chain breakage), which is indicated by a decrease in strength properties and an increase in the flow rate. On the other hand, the change of the screw configuration did not affect the oxidative degradation of PLA, which is confirmed by the results of the infrared and Raman analyses.

The addition of graphite has a slight influence on the mechanical properties and the melt flow rate of the obtained composites. For mechanical tests, a slight decrease in the measured values was noticed that is within the standard deviation of the measurement. Graphite filler improves the Charpy impact strength of composites. The MFR value slightly decreased after adding graphite to the polymer matrix.

The addition of graphite and the configuration of the type of extruder plasticizing system used had no effect on the thermal properties of the composites. There were no differences in the melting point and the degree of crystallinity of the tested samples. All samples showed an amorphous nature. The only observation worth noticing is the increase in enthalpy and the decrease in the cold crystallisation temperature of samples containing graphite microplates. This effect is related to the nucleophilic properties of the graphite filler.

The proposed configurations of the plasticizing system did not have a significant impact on the degradation of PLA and thus on the deterioration of the obtained composites' properties. At the same time, the K3 and K5 configurations made it possible to obtain samples with an excellent dispersion of the filler in the polymer matrix.

REFERENCES

1. Taib N-AAB, Rahman MR, Huda D, Kuok KK, Hamdan S, Bakri MKB, Julaihi MRMB, Khan A. A review on poly lactic acid (PLA) as a biodegradable polymer. Polym Bull, 2022.

2. Banerjee R, Ray SS. Sustainability and Life Cycle Assessment of Thermoplastic Polymers for Packaging: A Review on Fundamental Principles and Applications. Macromolecular Materials and Engineering, 2022; 307:2100794.

3. Siracusa V, Blanco I. Bio-Polyethylene (Bio-PE), Bio-Polypropylene (Bio-PP) and Bio-Poly(ethylene terephthalate) (Bio-PET): Recent Developments in Bio-Based Polymers Analogous to Petroleum-Derived Ones for Packaging and Engineering Applications. Polymers, 2020;12:1641.

4. Jenck JF, Agterberg F, Droescher MJ. Products and processes for a sustainable chemical industry: a review of achievements and prospects. Green Chem,2004; 6:544–556.

5. Kaplan DL. Introduction to Biopolymers from Renewable Resources. In: Kaplan DL (ed) Biopolymers from Renewable Resources. Springer, Berlin, Heidelberg, 1998; 1–29.

6. Kümmerer K. Sustainable from the very beginning: rational design of molecules by life cycle engineering as an important approach for green pharmacy and green chemistry. Green Chem, 2007; 9: 899–907.

7. Androsch R, Di Lorenzo ML. Synthesis, Structure and Properties of Poly(lactic acid), 1st ed. 2018.

8. Hu R-H, Ma Z-G, Zheng S, Li Y-N, Yang G-H, Kim H-K, Lim J-K. A fabrication process of high volume fraction of jute fiber/polylactide composites for truck liner. Int J Precis Eng Manuf, 2012;13: 1243–1246.

9. Notta-Cuvier D, Odent J, Delille R, Murariu M, Lauro F, Raquez JM, Bennani B, Dubois P. Tailoring polylactide (PLA) properties for automotive applications: Effect of addition of designed additives on main mechanical properties. Polymer Testing, 2014; 36:1–9.

10. Sevostyanov MA, Kaplan MA, Nasakina EO. Development of a Biodegradable Polymer Based on High-Molecular-Weight Polylactide for Medicine and Agriculture: Mechanical Properties and Biocompatibility. Dokl Chem, 2020; 490:36–39.

11. Tertyshnaya Y, Jobelius H, Olkhov A, Shibryaeva L, Ivanitskikh A. Polylactide Fiber Materials and their Application in Agriculture. Key Engineering Materials. 2022; 910:617–622.

12. Peres C, Matos AI, Conniot J, Sainz V, Zupančič E, Silva JM, Graça L, Sá Gaspar R, Préat V, Florindo HF. Poly(lactic acid)-based particulate systems are promising tools for immune modulation. Acta Biomaterialia, 2017; 48:41–57.

13. Sullivan MP, McHale KJ, Parvizi J, Mehta S. Nanotechnology. The Bone & Joint Journal, 2014; 96-B:569–573.

14. Zhou J, Yu J, Bai D, Lu J, Liu H, Li Y, Li L. AgNW/stereocomplex-type polylactide biodegradable conducting film and its application in flexible electronics. J Mater Sci: Mater Electron, 2021;32:6080–6093.

15. Al-Attar H, Alwattar AA, Haddad A, Abdullah BA, Quayle P, Yeates SG. Polylactide-perylene derivative for blue biodegradable organic light-emitting diodes. Polymer International, 2021; 70:51–58.

16. Ahmed J, Mulla M, Jacob H, Luciano G, T.b. B, Almusallam A. Polylactide/poly(ε-caprolactone)/zinc oxide/clove essential oil composite antimicrobial films for scrambled egg packaging. Food Packaging and Shelf Life, 2019; 21:100355.

17. Ahmed J, Mulla MZ, Al-Zuwayed SA, Joseph A, Auras R. Morphological, barrier, thermal, and rheological properties of high-pressure treated co-extruded polylactide films and the suitability for food packaging. Food Packaging and Shelf Life, 2022; 32:100812.

18. Raquez J-M, Habibi Y, Murariu M, Dubois P. Polylactide (PLA)-based nanocomposites. Progress in Polymer Science, 2013; 38:1504–1542.

19. Malinowski R, Raszkowska-Kaczor A, Moraczewski K, Głuszewski W, Krasinskyi V, Wedderburn L. The Structure and Mechanical Properties of Hemp Fibers-Reinforced Poly(ε-Caprolactone) Composites Modified by Electron Beam Irradiation. Applied Sciences, 2021; 11:5317.

20. Thakur KAM, Kean RT, Zupfer JM, Buehler NU, Doscotch MA, Munson EJ. Solid State 13C CP-MAS NMR Studies of the Crystallinity and Morphology of Poly(l-lactide). Macromolecules, 1996; 29:8844–8851.

21. Sinha Ray S, Yamada K, Okamoto M, Ueda K. New polylactide-layered silicate nanocomposites. 2. Concurrent improvements of material properties, biodegradability and melt rheology. Polymer, 2003; 44:857–866.

22. Fiedurek K, Szroeder P, Macko M, Raszkowska-Kaczor A, Puszczykowska N. Influence of the parameters of the extrusion process on the properties of PLA composites with the addition of graphite. IOP Conf Ser: Mater Sci Eng, 2021 1199:012057.

23. Gonçalves C, Gonçalves IC, Magalhães FD, Pinto AM. Poly(lactic acid) Composites Containing Carbon-Based Nanomaterials: A Review. Polymers,2017; 9:269.

24. Lim L-T, Auras R, Rubino M. Processing technologies for poly(lactic acid). Progress in Polymer Science,2008; 33:820–852.

25. Perepelkin KE. Polylactide Fibres: Fabrication, Properties, Use, Prospects. A Review. Fibre Chemistry, 2002; 34:85–100.

26. Harris AM, Lee EC. Improving mechanical performance of injection molded PLA by controlling crystallinity. Journal of Applied Polymer Science, 2018; 107:2246–2255.

27. Tümer EH, Erbil HY. Extrusion-Based 3D Printing Applications of PLA Composites: A Review. Coatings, 2021; 11:390.

28. Cicala G, Giordano D, Tosto C, Filippone G, Recca A, Blanco I. Polylactide (PLA) Filaments a Biobased Solution for Additive Manufacturing: Correlating Rheology and Thermomechanical Properties with Printing Quality. Materials, 2018; 11:1191.

29. Ghasem N, Al-Marzouqi M, Abdul Rahim N. Effect of polymer extrusion temperature on poly(vinylidene fluoride) hollow fiber membranes: Properties and performance used as gas–liquid membrane contactor for CO2 absorption. Separation and Purification Technology, 2012; 99:91–103.

30. Schweighuber A, Felgel-Farnholz A, Bögl T, Fischer J, Buchberger W. Investigations on the influence of multiple extrusion on the degradation of polyolefins. Polymer Degradation and Stability, 2021; 192:109689.

31. Kosmalska D, Janczak K, Raszkowska-Kaczor A, Stasiek A, Ligor T. Polylactide as a Substitute for Conventional Polymers—Biopolymer Processing under Varying Extrusion Conditions. Environments, 2022; 9:57.

32. Michael FM, Khalid M, Walvekar R, Ratnam CT, Ramarad S, Siddiqui H, Hoque ME. Effect of nanofillers on the physico-mechanical properties of load bearing bone implants. Materials Science and Engineering, 2016; C 67:792–806.

33. Pan J, Bian L. A physics investigation for influence of carbon nanotube agglomeration on thermal properties of composites. Materials Chemistry and Physics, 2019; 236:121777.

34. Tamayo-Vegas S, Muhsan A, Liu C, Tarfaoui M, Lafdi K. The Effect of Agglomeration on the Electrical and Mechanical Properties of Polymer Matrix Nanocomposites Reinforced with Carbon Nanotubes. Polymers, 2022; 14:1842.

35. Canevarolo SV, Babetto AC. Effect of screw element type in degradation of polypropylene upon multiple extrusions. Advances in Polymer Technology, 2002; 21:243–249.

36. Zou D, Zheng X, Ye Y, Yan D, Xu H, Si S, Li X. Effect of different amounts of bamboo charcoal on properties of biodegradable bamboo charcoal/polylactic acid composites. International Journal of Biological Macromolecules, 2022; 216:456–464.

37. Aversa C, Barletta M, Gisario A, Pizzi E, Prati R, Vesco S. Corotating twin-screw extrusion of poly(lactic acid) PLA/poly(butylene succinate) PBS/ micro-lamellar talc blends for extrusion blow molding of biobased bottles for alcoholic beverages. Journal of Applied Polymer Science, 2021 138:51294.

38. Kaczor D, Fiedurek K, Bajer K, Raszkowska-Kaczor A, Domek G, Macko M, Madajski P, Szroeder P. Impact of the Graphite Fillers on the Thermal Processing of Graphite/Poly(lactic acid) Composites. Materials, 2021; 14:5346.

39. Kaczor D, Bajer K, Domek G, Raszkowska-Kaczor A, Szroeder P. The method of obtaining polymer masterbatches based on polylactide with carbon filler. IOP Conf Ser: Mater Sci Eng, 2021; 1199:012058.

40. PN-EN ISO 11357-(1-3):2009 Tworzywa sztuczne - Różnicowa kalorymetria skaningowa (DSC) - Część 1: Zasady ogólne; Część 2: Wyznaczanie temperatury zeszklenia i stopnia przejścia w stan szklisty; Część 3: Oznaczanie temperatury oraz entalpii topnienia i krystalizacji.

41. Silva M, Gomes C, Pinho I, Gonçalves H, Vale AC, Covas JA, Alves NM, Paiva MC. Poly(Lactic Acid)/Graphite Nanoplatelet Nanocomposite Filaments for Ligament Scaffolds. Nanomaterials, 2021; 11:2796.

42. Batakliev T, Georgiev V, Kalupgian C, Muñoz PAR, Ribeiro H, Fechine GJM, Andrade RJE, Ivanov E, Kotsilkova R. Physico-chemical Characterization of PLA-based Composites Holding Carbon Nanofillers. Appl Compos Mater, 2021; 28:1175–1192.

43. PN-EN ISO 1133-1:2011 Tworzywa sztuczne - Oznaczanie masowego wskaźnika szybkości płynięcia (MFR) i objętościowego wskaźnika szybkości płynięcia (MVR) tworzyw termoplastycznych - Część 1: Metoda standardowa.

44. PN-EN ISO 294-1:2017-07 Tworzywa sztuczne - Wtryskiwanie kształtek do badań z tworzyw termoplastycznych - Część 1: Zasady ogólne, formowanie uniwersalnych kształtek do badań i kształtek w postaci beleczek.

45. PN-EN ISO 527-1:2020-01 Tworzywa sztuczne - Oznaczanie właściwości mechanicznych przy statycznym rozciąganiu - Część 1: Zasady ogólne.

46. PN-EN ISO 179-2:2020-12 Tworzywa sztuczne - Oznaczanie udarności metodą Charpy'ego - Część 2: Instrumentalne badanie udarności.

47. Yuniarto K, Purwanto YA, Purwanto S, Welt BA, Purwadaria HK, Sunarti TC. Infrared and Raman studies on polylactide acid and polyethylene glycol-400 blend. AIP Conference Proceedings, 2016; 1725:020101.

48. Kister G, Cassanas G, Vert M. Effects of morphology, conformation and configuration on the IR and Raman spectra of various poly(lactic acid)s. Polymer, 1998; 39:267–273.

49. Amorin NSQS, Rosa G, Alves JF, Gonçalves SPC, Franchetti SMM, Fechine GJM. Study of thermodegradation and thermostabilization of poly(lactide acid) using subsequent extrusion cycles. Journal of Applied Polymer Science, 2014 131, 40023.

50. Qin D, Kean RT. Crystallinity Determination of Polylactide by FT-Raman Spectrometry. Appl Spectrosc, 1998; 52:488–495.

51. Signori F, Coltelli M-B, Bronco S. Thermal degradation of poly(lactic acid) (PLA) and poly(butylene adipate-co-terephthalate) (PBAT) and their blends upon melt processing. Polymer Degradation and Stability, 2009; 94:74–82.

52. Cock F, Cuadri AA, García-Morales M, Partal P. Thermal, rheological and microstructural characterisation of commercial biodegradable polyesters. Polymer Testing, 2013; 32:716–723.

53. Carrasco F, Pagès P, Gámez-Pérez J, Santana OO, Maspoch ML. Processing of poly(lactic acid): Characterization of chemical structure, thermal stability and mechanical properties. Polymer Degradation and Stability, 2010; 95:116–125.

54. Mainil-Varlet P, Hauke C, Maquet V, Printzen G, Arens S, Schaffner T, Jérôme R, Perren S, Schlegel U. Polylactide implants and bacterial contamination: An animal study. Journal of Biomedical Materials Research, 2001; 54:335–343.

55. Usachev SV, Lomakin SM, Koverzanova EV, Shilkina NG, Levina II, Prut EV, Rogovina SZ, Berlin AA. Thermal degradation of various types of polylactides research. The effect of reduced graphite oxide on the composition of the PLA4042D pyrolysis products. Thermochimica Acta, 2022; 712:179227.

56. Mngomezulu ME, Luyt AS, John MJ. Morphology, thermal and dynamic mechanical properties of poly(lactic acid)/expandable graphite (PLA/EG) flame retardant composites. Journal of Thermoplastic Composite Materials, 2019; 32:89–107.

57. Harmandaris VA, Daoulas KCh, Mavrantzas VG. Molecular Dynamics Simulation of a Polymer Melt/Solid Interface: Local Dynamics and Chain Mobility in a Thin Film of Polyethylene Melt Adsorbed on Graphite. Macromolecules, 2005; 38:5796–5809.

58. Mysiukiewicz O, Barczewski M, Skórczewska K, Matykiewicz D. Correlation between Processing Parameters and Degradation of Different Polylactide Grades during Twin-Screw Extrusion. Polymers, 2020; 12:1333.

59. Przekop RE, Kujawa M, Pawlak W, Dobrosielska M, Sztorch B, Wieleba W. Graphite Modified Polylactide (PLA) for 3D Printed (FDM/FFF) Sliding Elements. Polymers, 2020; 12:1250.

60. Murariu M, Dechief AL, Bonnaud L, Paint Y, Gallos A, Fontaine G, Bourbigot S, Dubois P. The production and properties of polylactide composites filled with expanded graphite. Polymer Degradation and Stability, 2010; 95:889–900.

61. Żenkiewicz M, Richert J, Rytlewski P, Richert A. Comparative analysis of shungite and graphite effects on some properties of polylactide composites. Polymer Testing, 2011; 30:429–435.

62. Kim I-H, Jeong YG. Polylactide/exfoliated graphite nanocomposites with enhanced thermal stability, mechanical modulus, and electrical conductivity. Journal of Polymer Science Part B: Polymer Physics, 2010; 48:850–858.

63. Żenkiewicz M, Richert J, Rytlewski P, Moraczewski K, Stepczyńska M, Karasiewicz T. Characterisation of multi-extruded poly(lactic acid). Polymer Testing, 2009; 28:412–418.

Daniel Kaczor: https://orcid.org/0000-0002-0291-2121

Krzysztof Bajer: https://orcid.org/0000-0002-4719-5760

Grzegorz Domek: https://orcid.org/0000-0003-3566-9110

Piotr Madajski: https://orcid.org/0000-0002-6995-1643

Aneta Raszkowska-Kaczor: https://orcid.org/0000-0002-6868-6833

Paweł Szroeder: https://orcid.org/0000-0002-4266-4206